Research Article

Ghada ALMisned, Duygu Sen Baykal, Wiam Elshami, Gulfem Susoy, Gokhan Kilic, and Huseyin Ozan Tekin*

A comparative analysis of shielding effectiveness in glass and concrete containers

https://doi.org/10.1515/phys-2024-0019
received January 16, 2024; accepted April 10, 2024

Abstract: Nuclear waste control and related equipment play a vital role in safeguarding human health and the environment from the potential dangers of radioactive waste. This study addresses the critical challenge of enhancing the shielding effectiveness of container materials for nuclear waste management, with a focus on comparing the attenuation properties of glass and concrete composites. Our analysis revealed that the copper oxide-reinforced borosilicate glass container demonstrated a significant transmission factor (TF) value decrease by approximately 15% compared to steel–magnetite concrete at 1.3325 MeV, with a standard deviation of ±1.5%, indicating its lower protective characteristics. Nonetheless, it exhibited a 10% higher TF reduction compared to the cement–bitumen mix at the same energy level, with a precision error of ±1.2%. In addition, the half-value layer for this glass was determined to be 2.5 cm for 1.3325 MeV gamma rays, showing moderate shielding capacity. The study demonstrates that optimizing the oxide content in the borosilicate glass matrix significantly enhances its shielding effectiveness. This advancement in nuclear waste management materials is justified by our comprehensive evaluation, highlighting the potential of optimized glass materials to outperform traditional concrete in certain scenarios, thus contributing to the development of more effective nuclear waste containment solutions.

Keywords: material properties, nuclear waste management, container, Monte Carlo simulations

*** Corresponding author: Huseyin Ozan Tekin**, Department of Medical Diagnostic Imaging, College of Health Sciences, University of Sharjah, 27272, Sharjah, United Arab Emirates; Computer Engineering Department, Faculty of Engineering and Natural Sciences, Istinye University, Istanbul 34396, Turkey, e-mail: tekin765@gmail.com
Ghada ALMisned: Department of Physics, College of Science, Princess Nourah Bint Abdulrahman University, P.O. Box 84428, Riyadh 11671, Saudi Arabia
Duygu Sen Baykal: Faculty of Engineering and Architecture, Mechatronics Engineering, Istanbul Nisantasi University, Istanbul 34398, Turkey
Wiam Elshami: Department of Medical Diagnostic Imaging, College of Health Sciences, University of Sharjah, 27272, Sharjah, United Arab Emirates
Gulfem Susoy: Department of Physics, Faculty of Science, Istanbul University, Istanbul 34134, Turkey
Gokhan Kilic: Department of Physics, Faculty of Science, Eskisehir Osmangazi University, Eskisehir TR-26040, Turkey

1 Introduction

The management of nuclear waste is critically important due to the dangerous residual materials produced by nuclear power generation, research, and other nuclear-related activities [1,2]. The disposal of such waste is a major concern, as radioactive substances can pose long-term risks to human health and the environment, potentially lasting thousands of years [3]. Ensuring the safe handling and storage of this waste is, therefore, essential. Radioactive materials are known to cause significant health hazards, including cancer and genetic mutations, due to the emission of ionizing radiation [4]. Effective management practices are crucial for securely confining and segregating radioactive waste, thereby minimizing its impact on both humans and ecosystems [5]. Some radioactive isotopes in nuclear waste can remain hazardous for many years [6], making efficient waste management strategies imperative to protect future generations from the consequences of poorly managed waste [7]. Moreover, securely storing and monitoring this waste can mitigate risks associated with accidental releases or contamination. There is also a concern that nuclear waste could be used to develop nuclear weapons if mismanaged or diverted. Implementing effective management practices reduces the risk of unauthorized access to nuclear materials, thus helping to prevent nuclear proliferation and enhance global security [8]. Nuclear waste containers play a pivotal role in waste management, serving as specialized receptacles for storing and transporting radioactive materials from nuclear power plants and other related facilities [8]. Recent advancements in nuclear waste management have been significantly influenced by innovative material studies. Eskander *et al.* [9] explored the potential of cement–polymer composites, particularly those based on recycled polystyrene foam wastes, for

construction applications and their interaction with water ecologies. Saleh *et al.* [10] advanced this field by blending asphaltene or polyvinylchloride waste with cement, creating sustainable materials applicable in nuclear safety contexts. Further exploring material efficacies, Saleh *et al.* [11] investigated the consistency and gamma-radiation shielding efficiency of cement–bitumen composites, presenting a viable option for radiation protection. In another study, Saleh *et al.* [12] conducted mechanical and physicochemical evaluations of solidified dried submerged plants under extreme climatic conditions, aiming for optimal waste containment solutions. The exploration of optical properties and gamma radiation shielding capabilities of transparent barium borosilicate glass composites by Ehab *et al.* [13] marked a significant stride in using glass materials for radiation protection. Finally, Eid *et al.* [14] examined the impact of gamma and neutron irradiation on Portland cement integrated with waste silicate glass, contributing to our understanding of the durability and performance of cement-based materials in nuclear waste applications. These studies collectively represent substantial progress in the development of novel and sustainable materials, underpinning the ongoing evolution of nuclear waste management strategies. The nuclear waste containers are designed to securely confine radioactive waste and protect against radiation risks. Typically made from durable materials like steel, concrete, or lead (Pb), these containers must possess strong shielding properties to effectively contain radiation [15]. It is also vital to ensure that these containers are hermetically sealed to prevent the leakage of radioactive materials. Advanced leak detection systems are often used to monitor for any potential breaches. In recent years, there has been an increasing interest in using heavy glass for containing radioactive materials, as it offers several advantages over traditional materials like concrete, which can suffer from corrosion, structural deformations, and compromised integrity due to moisture [16–18]. Glass materials, known for their exceptional properties, are being considered for the safe storage of nuclear waste over extended periods [19–23]. The scientific community is exploring the use of glass in nuclear waste management, driven by the potential of these materials to effectively counteract various hazards through vitrification. This investigation focuses on the behaviour of copper(II) oxide-doped C8(BCV0.5) glass [24], a material synthesized and analysed by our research team, in the context of a nuclear waste container. We conducted a comparative evaluation of the shielding effectiveness of various container types, including lead-added glass containers, 0.5 cement–0.5 bitumen [25], and steel–magnetite concrete [26]. The primary objective of this investigation is to conduct a thorough evaluation of the shielding effectiveness of glass and concrete containers, employing radioisotope energies of ^{60}Co and ^{137}Cs, for nuclear waste management applications. A distinctive focus of our research is the comparative analysis of traditional materials, such as steel–magnetite concrete, with innovative glass composites, specifically copper oxide-reinforced borosilicate glass.

2 Materials and methods

In this study, the first phase began with the selection of diverse materials for their potential applications as nuclear waste containers, including both conventional options and our novel copper oxide-reinforced borosilicate glass. By utilizing the Monte Carlo N-Particle Transport (MCNP) 6.3 code, we simulated and analysed the shielding effectiveness of each material, focusing on transmission factors (TFs) and energy deposition.

2.1 C8 (BCV0.5) glass sample: Fabrication and main properties

The $55B_2O_3$–$35CaO$–$9Al_2O_3$–$0.5CuO$–$0.5V_2O_5$ glass structure [24] was used to create the C8 (BCV0.5) glass sample using the melt-quenching technique. In a platinum crucible heated to 900°C, a sample of C8 (BCV0.5) was melted using high-purity chemicals. The sample (Figure 1) was then subjected to an annealing procedure to achieve an equilibrium of internal forces at a temperature estimated to be 385°C. Weighing equipment was used to accurately measure each oxidized chemical. The high-

Figure 1: Physical appearance of the synthesized Copper(II) oxide reinforced glass sample BCV0.5.

temperature furnace was gradually heated to a temperature of 900°C during the first hour of the procedure. At this point, mechanical stirring was carried out every 15 min. The glass sample was transformed into the desired configuration after being liquefied, and the sample underwent an annealing process for roughly an hour at a temperature range of 380–385°C. The sample was then cooled to room temperature. For detailed information on the physical and technical properties of the synthesized glass sample, readers are referred to the comprehensive analysis provided in the study by Ilik *et al.* [24].

2.2 Designing container geometry

The utilization of MCNP 6.3 software [27], widely used for modelling radiation transport in complex geometries and systems, enables the creation of intricate geometric configurations crucial for ensuring the effectiveness and proficiency of container materials. The initial step in using MCNP for container material design involves generating a 3D model of the container, which accurately represents the physical attributes of the material and its components. The software then uses mathematical algorithms to simulate the behaviour of the container material under various conditions. The precise definition of geometry plays a key role in determining the accuracy and quality of the simulation. Once created, the geometry is assigned specific materials and placed within the simulated system. Figure 2 depicts the transportable container model in a 2D representation, relevant to this project. The coordinates (0, 0, 0) indicate the placement of an isotropic point source at the centre of the simulation volume. For the glass and concrete containers, distinct chemical compositions were used to create unique cell structures, aimed at producing portable containers. An air cell was incorporated around the glass container to allow for accurate measurement of energy released into the adjacent air compartment, with a protective attenuator layer isolating the air compartment from external elements, as shown in Figure 3. This investigation modelled the emission of radiation into four different vessels, utilizing energy from the radioactive decay of ^{60}Co and ^{137}Cs isotopes within the containers. To ensure the integrity of the surrounding air in the event of a radiation release, six NaI (Tl) scintillation detectors, each measuring 3 × 3 inches, were strategically placed across the simulation zones (Figure 4). These detectors, labelled a through f, were used to assess the effectiveness of the air environment's sealing around the container and to confirm that the measured air-kinetic energy released per unit mass (KERMA) is representative of the actual ambient air near the container.

2.3 Simulation phase

The determination of the TF values, which is a crucial parameter utilized in the assessment of shielding effectiveness, for a specific substance provides valuable information regarding the degree of absorption that can be attributed to that substance. Therefore, the Monte Carlo MCNP code for the C8 (BCV0.5) glass sample simulated the TF. The gamma-ray TF

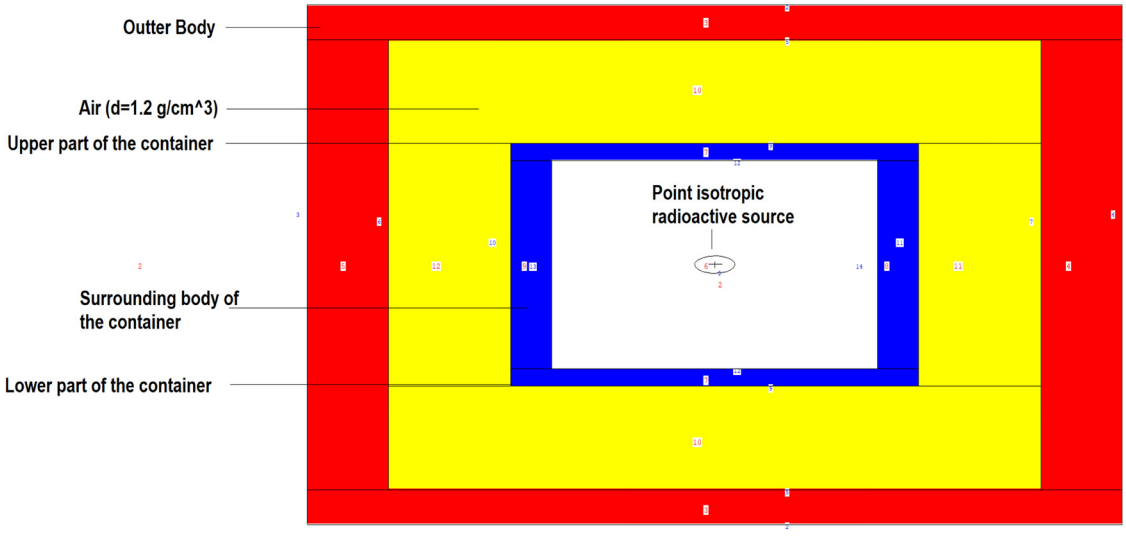

Figure 2: 2-D view of modelled glass container along with the surrounding air environment and the point radioactive isotope obtained through MCNP Visual Editor.

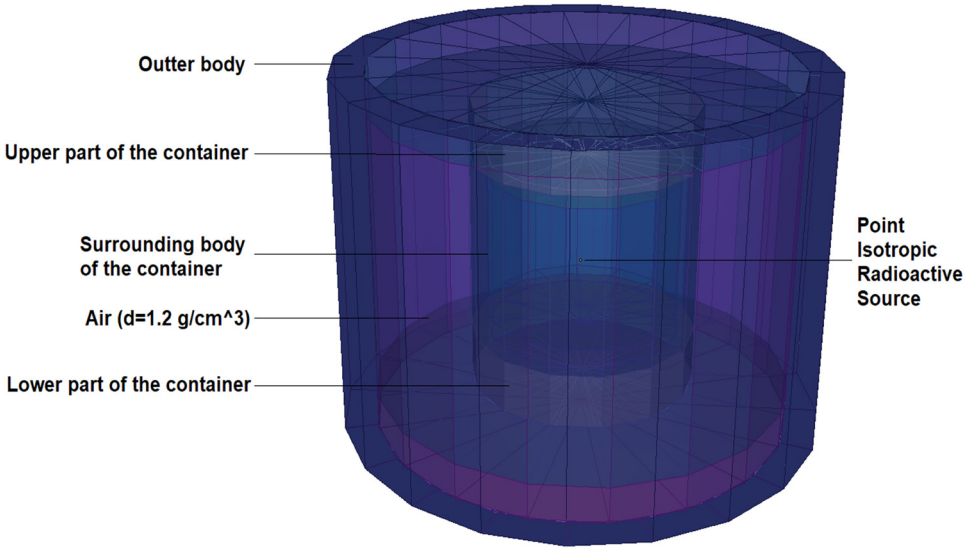

Figure 3: 3-D view of modelled glass container along with the surrounding air environment and the point radioactive isotope obtained through MCNP Visual Editor.

(%) is a crucial metric in the assessment of materials used for radiation shielding, particularly in the context of nuclear waste management. This factor quantifies the percentage of gamma radiation that penetrates a material, providing insights into the material's effectiveness in blocking radiation. The lower the TF, the more effective the material is at attenuating gamma rays.

$$\text{Transmission factor (TF)}: \left(\frac{I_0}{I}\right). \tag{1}$$

In Eq. (1), I is the intensity of the gamma radiation after passing through the shielding material and I_0 is the original intensity of the gamma radiation before encountering the material [28]. The obtained TF results are subsequently compared to those of traditional shielding materials, which were assessed using identical criteria. The designed container structures were initially evaluated according to the elemental characteristics of the input file of the MCNP code (Table 1). The densities of these structures were also included in the input file. The procurement of primary and secondary gamma-ray fluxes was subsequently achieved through the establishment of two detection regions with identical dimensions, positioned directly in front of and behind the absorber material. The procedure in question is implemented through

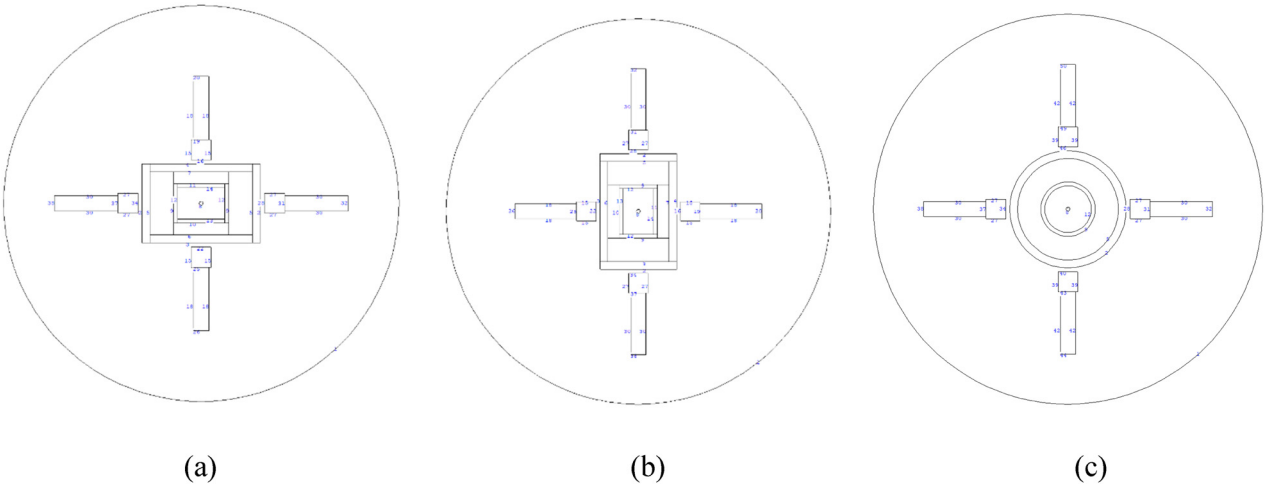

Figure 4: (a–c) 2-D representation of the modeled nuclear container as obtained through the MCNP Visual Editor: (a) horizontal-lateral view, (b) vertical-lateral view, and (c) top view.

Table 1: Sample codes, elemental weight fractions and densities of C8 (BCV0.5), concrete (Steel–Magnetite); 0.5 Cement–0.5 Bitumen, U (Pb composite glass) glasses

Samples code	Elemental weight fraction (wt%)											Density, ρ (g/cm^3)
	He	**C**	**N**	**O**	**Na**	**Al**	**Si**	**S**	**K**	**Ca**	**Fe**	
0.5 Cement–0.5 Bitumen	0.08642	0.1874	0.07855	0.33456	0.00650	0.01373	0.04406	0.0255	0.0008	0.19741	0.02507	2.600
C8 (BCV0.5)	**B**	**O**	**Al**	**Ca**	**V**	**Cu**	—	—	—	—	—	3.003
	0.17081	0.52462	0.04763	0.25014	0.0028	0.0040	—	—	—	—	—	
U (Pb composite glass)	**O**	**Na**	**Si**	**K**	**Zn**	**Pb**	—	—	—	—	—	
	0.36497	0.01484	0.28046	0.09962	0.00803	0.23208	—	—	—	—	—	4.356
Concrete (Steel–Magnetite)	**H**	**O**	**Mg**	**Al**	**Si**	**P**	**S**	**Ca**	**Mn**	**Fe**	—	5.11
	0.00510	0.15697	0.00580	0.00660	0.02679	0.00080	0.00060	0.03949	0.00070	0.75715	—	

the utilization of the F4 designation within the MCNP programming language. A location preceding the absorber glass material and the initial detection region was identified as the source of isotropic behaviours emanating from a point source. The determination of the characteristic energy of gamma rays was carried out for each cycle of simulation, relying on the provided source description. The research utilized MCNP simulations through the implementation of the D00205ALLCP03 MCNPDATA package, which incorporates the DLC-200/MCNPDATA cross-section libraries. In the simulation phase, we utilized a Lenovo P620 workstation, chosen for its robust performance capabilities, which are essential for handling the computationally intensive tasks involved in Monte Carlo simulations. The workstation is powered by an AMD Ryzen Threadripper PRO 3945WX processor with 12 cores, providing the necessary computational power to efficiently process large data sets and complex calculations. It is equipped with 64 GB of RAM, ensuring smooth data processing and simulation runs. The system also includes an NVIDIA Quadro P2200 graphics card, which supports the high-resolution visualizations required for our study. The workstation runs on a Windows 10 Pro operating system, offering a stable and secure platform for our simulations. This hardware configuration, combined with the advanced features of the Monte Carlo N-Particle Transport Code, version 2.7.0, enabled precise and reliable simulation results, contributing significantly to the robustness and accuracy of our study's findings.

3 Results and discussion

The present investigation assessed the efficacy of four distinct containers in protecting against gamma radiation. The containers were designed and subsequently compared in three distinct phases. The initial phase of the analysis involved comparing the TF obtained for the materials specified in the container concept. The TF represents the proportionality between the photon beam that traverses a material cross section and arises on the opposite side, and the attenuation of the primary photon beam due to interaction with the material [29]. Given that the primary photon beam's intensity remains constant across different materials owing to the source, the sole variable that will vary based on material properties is the intensity of the secondary photon beam. The quantitative properties of the secondary photon beam and the proportional differences between the intensities of the primary and secondary photon beams are determined by the amount of attenuation that the beam undergoes as it passes through the material. The decrease in the intensity of secondary photon beams will result in an overall decrease in the total TF value. The TF values acquired from ^{60}Co and ^{137}Cs sources are displayed in Figure 5, with respect to the progressively increasing material thickness for each container material. The figure illustrates that the TF values exhibit a decreasing trend at every energy level, which is dependent on the progressive increase in the thickness value of each container. The rationale behind this phenomenon can be elucidated by the observation that primary photons are susceptible to greater absorption within the material, contingent upon the progressive augmentation of material thickness. The study found that the minimum TF values were observed for a thickness of 3 cm, with material thicknesses ranging from 0.5 to 3 cm. Moreover, it is evident from the data presented in Figure 5 that the computation of TF values was examined across three distinct radioisotope energies, namely, 0.662, 1.1732, and 1.3325 MeV. The obtained TF values were observed to increase with the increase in energy, for a given thickness, based on the energy level. This phenomenon can be attributed to the relationship between the energy value

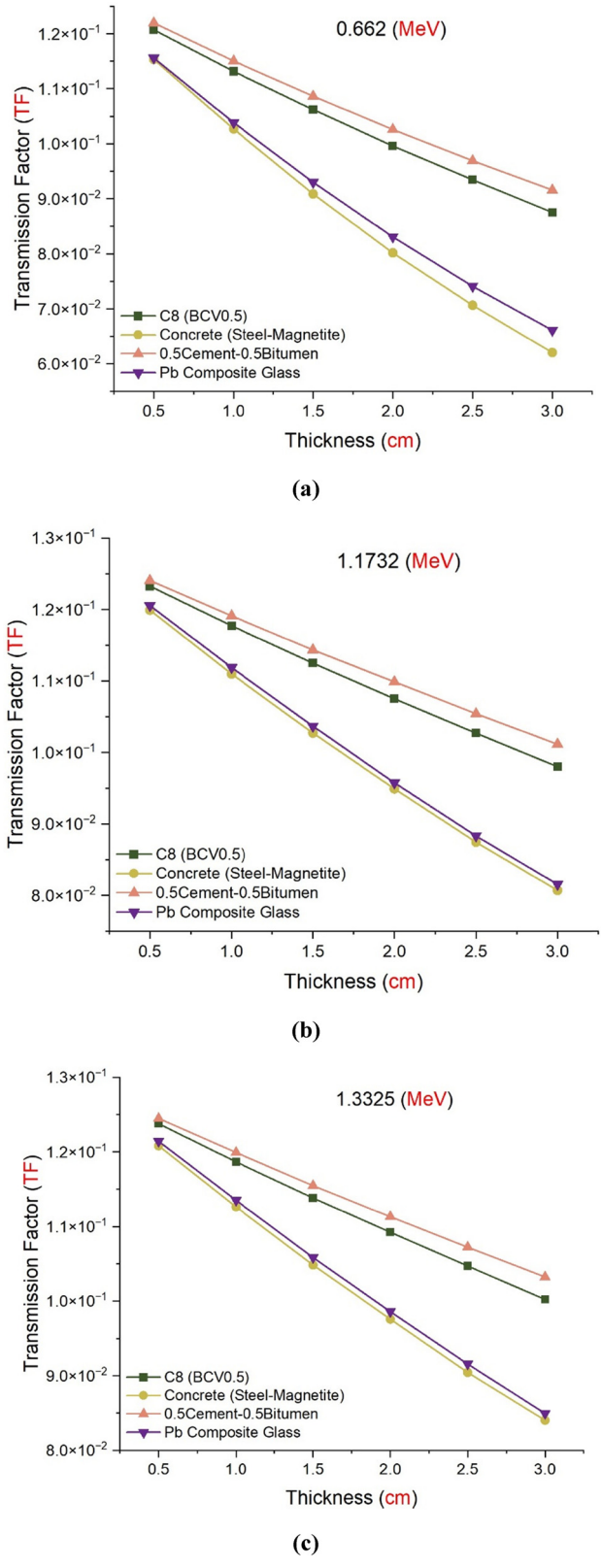

Figure 5: (a–c) Comparison of the TFs as a function of used radioisotope energies such as (a) 0.662 MeV, (b) 1.1732 MeV, (c) 1.3325 MeV for different glass thicknesses.

and the penetration properties of the photons [30–34]. As the energy value increases, the penetration properties also increase, leading to a decrease in the emitted energy per unit distance. Consequently, this results in an increase in the quantity of secondary photon beams. Of all the container materials examined, steel–magnetite concrete exhibited the lowest TF values. Subsequently, Pb composite glass, BCV0.5, and 0.5 cement–0.5 bitumen containers were utilized in accordance with this pattern. The dissimilarity is associated with the densities of materials, whereby the absorption properties of gamma-rays are known to be intimately linked with material density. The container doped with copper(II) oxide in BCV0.5 exhibited better protective characteristics in comparison to the container composed of 0.5 cement–0.5 bitumen. It is noteworthy that the TF values acquired are being compared based on identical thickness values. Hence, it is plausible that an increase in thickness of the BCV0.5 material could potentially lead to a decrease in TF values, resulting in values comparable to those observed in steel–magnetite concrete and Pb composite glass containers. During the second phase of the investigation, the half-value layer (HVL) values of the examined container materials were computed. The objective of the second phase was to conduct a comparative analysis between the simulation-based TF values obtained in the first phase and the theoretically derived HVL values. The HVL value represents a physical quantity that denotes the thickness (in centimetres) of a material necessary to halve a photon beam with a specific energy value in a quantitative manner [35]. Consequently, it can be posited that the material exhibiting a lower HVL value for a given energy level possesses superior radiation attenuation characteristics. The graphical representation depicted in Figure 6 illustrates the fluctuations in HVL measurements as a function of escalating energy levels for the four distinct materials of the containers that were examined. The figure illustrates a positive correlation between the energy value and HVL values, indicating an increase in the latter as the former increases. The rationale behind this is the requirement for increased thickness of the gamma ray beam, which exhibits enhanced penetration characteristics proportional to its energy level, to achieve a quantitative reduction of one-half in the material. To clarify, gamma rays possessing greater penetration exhibit an increased proclivity to traverse through matter due to their lower energy release per unit distance, resulting in reduced attenuation. On the other hand, Figure 6 illustrates a high degree of compatibility between the HVL and TF values obtained from the data. The steel–magnetite concrete material exhibited the lowest values for the TF metric as calculated through the employment of the MCNP computational tool. In addition, this

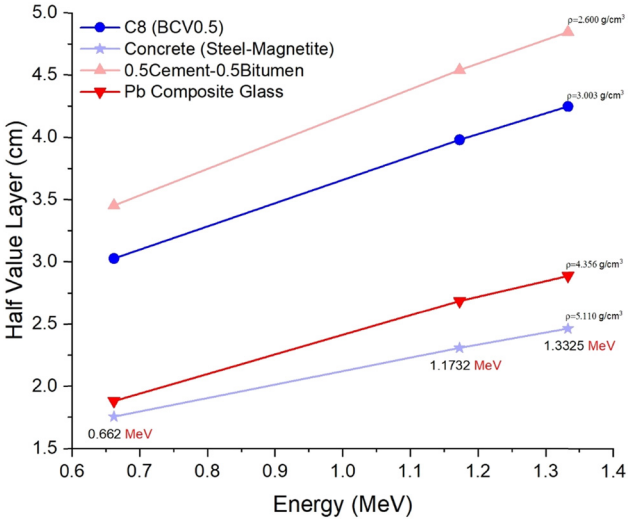

Figure 6: Variation of half value layer (cm) with photon energy (MeV) for C8 (BCV0.5), Concrete (Steel–Magnetite), 0.5 Cement–0.5 Bitumen and Pb Composite Glass.

material demonstrated a decreasing trend in HVL values. Upon close examination of the *y*-axis of the graph, it can be observed that there exists a twofold discrepancy between the steel–magnetite concrete and the BCV0.5 container with respect to the calculated HVL values. This pertains to the observation that doubling the thickness of the BCV0.5 container material during production will result in comparable absorption properties. That is, an absolute thickness increase is required in the BCV0.5 glass to provide the properties of steel–magnetite concrete for absorption properties. The augmentation may be achieved not only solely through an escalation in thickness, but also through an augmentation in the quantity of copper(II) oxide incorporated into the BCV0.5 glass. During the final phase of the investigation, the quantity of energy that was deposited in the air volume surrounding the designated containers was computed individually. As previously stated, and illustrated in Figure 3, the receptacle was charged with a volume of air, which was then encompassed by an external surface. Consequently, the linkage between the internal air atmosphere and the external environment was severed. The verification of the lack of any outward air leakage was conducted utilizing six distinct detectors, as illustrated in Figure 4. During this phase of the study, the objective was to determine the quantity of energy that was deposited because of the KERMA that occurred within the specified volume of air. The augmentation in the magnitude of gamma rays that traverse the surfaces of the container and enter the surrounding air will result in an elevation of the KERMA value, as it will lead to a greater degree of ionization within this particular volume of air. Consequently, it is anticipated that the quantity of energy discharged within the airspace encompassing the receptacle, which has greater surface gamma ray transmission, will be elevated. The occurrence of any absorption deficiency in the cone section will result in an elevation of the quantity of gamma rays assimilated into the air volume, leading to a corresponding increase in the level of ionization. The present scenario necessitates a meticulous evaluation with regards to safeguarding against radiation. The rationale behind this is that the dosimeters employed in quantifying the level of radiation exposure in occupational settings operate based on the magnitude of exposure in the atmosphere. Hence, the potential health hazards are likely to be greater in an atmosphere that is subject to increased exposure. This scenario warrants consideration with regards to the soil in which the containers will be situated. Figure 7 presents a critical visual representation of energy deposition in air as a gradient of colours, where warmer colours indicate higher gamma radiation exposure. This graphical illustration serves as a quantitative map, highlighting the variation in radiation containment capabilities of the different materials. In particular, the stark contrast in colour gradients between the container types provides an immediate visual cue to the relative performance of each material in shielding against gamma radiation. Upon closer examination of Figure 7, we note that the container composed of a 0.5 cement/0.5 bitumen mixture (a) exhibits a gradient with a substantial portion in red, signifying a higher degree of energy transmission and subsequent air exposure. This visualization corresponds quantitatively with the recorded TF and HVL values, where this material combination demonstrated the least effectiveness in radiation shielding. In stark contrast, the steel–magnetite concrete container (d) shows a predominantly green spectrum, indicating minimal energy deposition in the air above the container, which corroborates its superior shielding properties as reflected in the lowest TF and HVL values among the materials tested. The gradation from green to red in the colour spectrum effectively conveys the relative efficiency of the containment materials. The images in Figure 7 serve not only as a validation of the quantitative data obtained but also emphasize the practical implications of these findings in terms of environmental safety. The degree of redness, especially noted in the upper layers of the colour spectrum, can be directly correlated with the potential risk of gamma-ray leakage and its impact on the environment, which is a significant consideration in the storage and transportation of nuclear waste. The detailed observation of these colour gradients reveals nuanced differences in the materials' shielding behaviour, providing an intuitive understanding that complements the numerical data. The variation in colour intensity underscores the potential of copper(II) oxide-reinforced BVC0.5 glass (b) to enhance

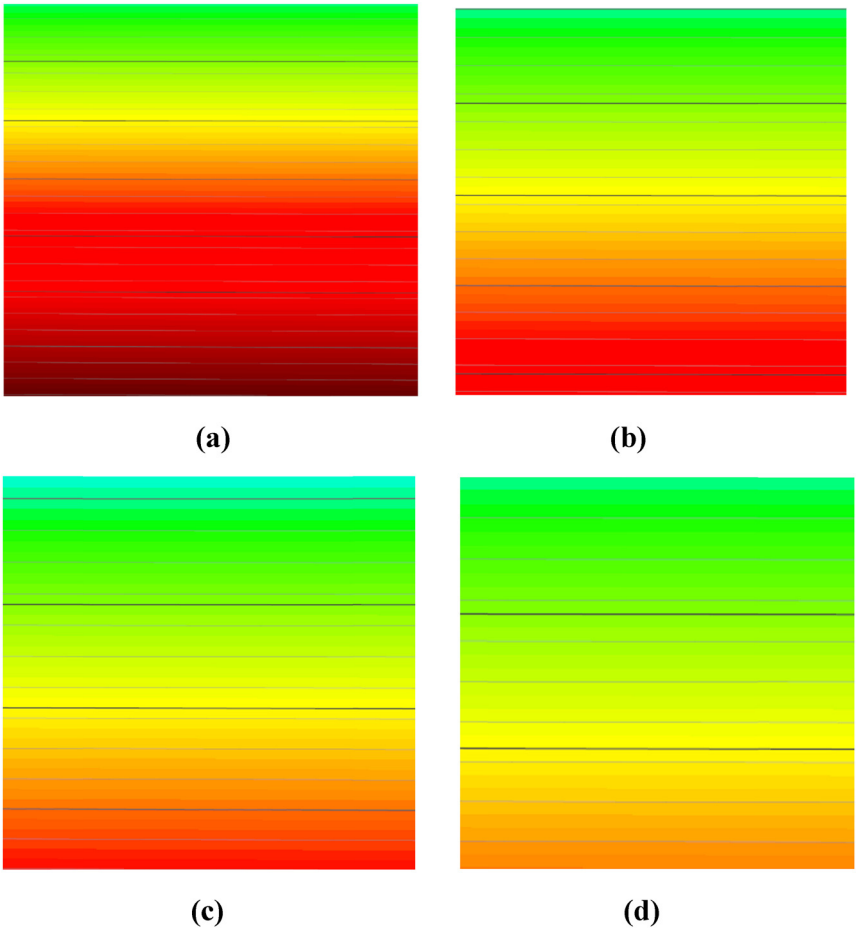

Figure 7: Distance-dependent cross-sectional color distribution of the energy in the air for (a) 0.5 Cement–0.5 Bitumen, (b) BCV0.5, (c) Pb Glass Composite, and (d) Concrete (Steel–Magnetite).

radiation protection, although not to the extent of traditional materials like steel–magnetite concrete, as evidenced by a more yellowish transition in the gradient. This finding adds a new dimension to our comparative analysis by visually and quantitatively establishing the intermediate shielding performance of our novel glass composite. Our findings suggest that while copper(II) oxide glass shows lower protective characteristics compared to steel–magnetite concrete, it notably outperforms other materials like the 0.5 cement–0.5 bitumen container. This insight opens new avenues for exploring glass-based materials in nuclear waste containment, a field traditionally dominated by concrete and steel materials. In addition, our research methodology, centred around the MCNP simulation, serves as a benchmark for future studies in this domain. By leveraging this advanced simulation technique, we were able to accurately model and analyse the behaviour of different container materials under various conditions, providing a level of detail and accuracy not commonly seen in traditional experimental approaches. The implications of this methodology extend beyond our specific findings, suggesting a new standard for material assessment in radiation safety applications. In conclusion, the significance of our research lies in its potential to influence the selection of materials for nuclear waste containment, guiding industry towards safer and more efficient practices. By providing new insights into the comparative effectiveness of different container materials, we contribute to the ongoing efforts to mitigate the environmental and health risks associated with nuclear waste, thereby playing a crucial role in the sustainable advancement of nuclear technology.

4 Conclusion

This investigation affirms the critical role of nuclear waste management in safeguarding public health and environmental safety. Our comparative study, utilizing radioisotope energies of ^{60}Co and ^{137}Cs, reveals that while copper oxide-infused borosilicate glass (BCV0.5) does not match

the shielding effectiveness of steel–magnetite concrete, it does outperform the 0.5 cement/0.5 bitumen mix. The presence of copper oxide enhances the radiation absorption of BCV glass, suggesting that increasing the oxide content could further improve its protective characteristics. Our findings, validated by the MCNP simulations in alignment with theoretical HVL values, provide a benchmark for future development of glass composites for nuclear waste containers. This research contributes to the field by offering new insights into the potential of glass-based materials in nuclear waste management, positioning copper oxide-doped glass as a promising alternative to traditional materials. In advancing the field of nuclear waste management, this study introduces a novel application of the MCNP code by specifically focusing on the optimization of glass composite materials for radiation shielding. While MCNP has been extensively used for various applications within nuclear science, its application in the comparative analysis of copper oxide-reinforced borosilicate glass and conventional materials for nuclear waste containment is a unique aspect of our research. Moreover, the proposed model offers the advantage of accurately simulating the shielding effectiveness of various container materials, allowing for a detailed comparison of traditional and novel composites under standardized conditions. However, its primary limitation lies in the extrapolation of simulated data to real-world scenarios, which may necessitate further empirical validation to account for environmental and operational variables not fully replicated in simulation environments. Looking forward, we envision expanding this line of research to explore the integration of nanotechnology in the synthesis of glass composites, aiming to further enhance their shielding effectiveness against a broader spectrum of radioactive emissions. In addition, assessing the long-term durability and environmental impact of these novel materials in real-world nuclear waste management scenarios represents a critical next step in validating their practical utility and sustainability.

Acknowledgments: The authors would like to express their deepest gratitude to Princess Nourah bint Abdulrahman University Researchers Supporting Project number (PNURSP2024R149), Princess Nourah bint Abdulrahman University, Riyadh, Saudi Arabia.

Funding information: Princess Nourah bint Abdulrahman University Researchers Supporting Project number (PNURSP2024R149), Princess Nourah bint Abdulrahman University, Riyadh, Saudi Arabia.

Author contributions: Ghada ALMisned: conceived and designed the experiments; performed the experiments; contributed reagents, materials, analysis tools or data; wrote the paper. Gokhan Kilic: performed the experiments; analysed and interpreted the data; contributed reagents, materials, analysis tools, or data. Duygu Sen Baykal: performed the experiments; analysed and interpreted the data. Wiam Elshami: contributed reagents, materials, analysis tools, or data. Huseyin Ozan Tekin: contributed reagents, materials, analysis tools, or data; performed the experiments; wrote the paper. All authors have accepted responsibility for the entire content of this manuscript and approved its submission.

Conflict of interest: The authors state no conflict of interest.

Data availability statement: The datasets generated during and/or analysed during the current study are available from the corresponding author on reasonable request.

References

[1] Ojovan MI, Steinmetz HJ. Approaches to disposal of nuclear waste. Energies. 2022;15(20):7804. doi: 10.3390/en15207804.
[2] Forsberg CW. Radioactive wastes. In: Meyers RA, editor. Encyclopedia of physical science and technology. 3rd edn. Academic Press; 2003. p. 643–59. doi: 10.1016/B0-12-227410-5/00642-6.
[3] Ewing RC, Meldrum A, Wang L, Weber WJ, Corrales LR. Environmental impacts of the long-term storage of spent nuclear fuel. Nat Mater. 2004;3(2):129–37.
[4] Ostad-Ali-Askari K. Management of risks substances and sustainable development. Appl Water Sci. 2022;12(4):65. doi: 10.1007/s13201-022-01599-6.
[5] El-Guebaly L. Managing fusion radioactive materials: Approaches and challenges facing fusion in the 21st century. Fusion Sci Technol. 2023;79(8):919–31. doi: 10.1080/15361055.2023.2161891.
[6] Rao KR. Radioactive waste: The problem and its management. Curr Sci. 2001;81(12):1534–46.
[7] Misra V, Pandey SD. Hazardous waste, impact on health and environment for development of better waste management strategies in future in India. Environ Int. 2005;31(3):417–31. doi: 10.1016/j.envint.2004.08.004.
[8] Nagasaki S, Nakayama S, editors. Radioactive waste engineering and management. Japan, Tokyo: Springer; 2015. doi: 10.1007/978-4-431-55651-3.
[9] Eskander SB, Saleh HM, Tawfik ME, Bayoumi TA. Towards potential applications of cement-polymer composites based on recycled polystyrene foam wastes on construction fields: Impact of exposure to water ecologies. Case Stud Constr Mater. 2021;15:e00664. doi: 10.1016/j.cscm.2021.e00664.
[10] Saleh HM, Bondouk II, Salama E, Mahmoud HH, Omar K, Esawii HA. Asphaltene or polyvinylchloride waste blended with cement to produce a sustainable material used in nuclear safety. Sustainability. 2022;14(6):3525. doi: 10.3390/su14063525.
[11] Saleh HM, Bondouk II, Salama E, Esawii HA. Consistency and shielding efficiency of cement-bitumen composite for use as gamma-radiation shielding material. Prog Nucl Energy. 2021;137:103764. doi: 10.1016/j.pnucene.2021.103764.

[12] Saleh HM, Moussa HR, El-Saied FA, Dawoud M, Bayoumi TA, Abdel Wahed RS. Mechanical and physicochemical evaluation of solidified dried submerged plants subjected to extreme climatic conditions to achieve an optimum waste containment. Prog Nucl Energy. 2020;122:103285. doi: 10.1016/j.pnucene.2020.103285.
[13] Ehab M, Salama E, Ashour A, Attallah M, Saleh HM. Optical properties and gamma radiation shielding capability of transparent barium borosilicate glass composite. Sustainability. 2022;14(20):13298. doi: 10.3390/su142013298.
[14] Eid MS, Bondouk II, Saleh HM, Omar KM, Diab HM. Investigating the effect of gamma and neutron irradiation on Portland cement provided with waste silicate glass. Sustainability. 2023;15(1):763. doi: 10.3390/su15010763.
[15] Gentry RV, Sworski TJ, McKown HS, Smith DH, Eby RE, Christie WH. Differential lead retention in zircons: implications for nuclear waste containment. Science. 1982;216(4543):296–8. doi: 10.1126/science.216.4543.296.
[16] ALMisned G, Tekin HO, Issa SA, Ersundu MÇ, Ersundu AE, Kilic G, et al. Novel HMO-glasses with Sb2O3 and TeO2 for nuclear radiation shielding purposes: a comparative analysis with traditional and novel shields. Materials. 2021;14(15):4330. doi: 10.3390/ma14154330.
[17] Tekin HO, ALMisned G, Zakaly HM, Zamil A, Khoucheich D, Bilal G, et al. Gamma, neutron, and heavy charged ion shielding properties of Er^{3+} -doped and Sm^{3+} -doped zinc borate glasses. Open Chem. 2022;20(1):130–45. doi: 10.1515/chem-2022-0059.
[18] Kurniawan TA, Othman MH, Singh D, Avtar R, Hwang GH, Setiadi T, et al. Technological solutions for long-term storage of partially used nuclear waste: A critical review. Ann Nucl Energy. 2022;166:108736. doi: 10.1016/j.anucene.2021.108736.
[19] Alsaif NA, Baykal DS, Elshami W, Zakaly HM, Issa SA, Ene A, et al. On tungsten barium phosphate glasses: Elastic moduli, gamma-ray shielding properties as well as transmission factor (TF). J Aust Ceram Soc. 2023;59(4):1095–109. doi: 10.1007/s41779-023-00998-9.
[20] Deliormanlı AM, Ensoylu M, Issa SA, Elshami W, Al-Baradi AM, Al-Buriahi MS, et al. WS2/bioactive glass composites: Fabrication, structural, mechanical and radiation attenuation properties. Ceram Int. 2021;47(21):29739–47. doi: 10.1016/j.ceramint.2021.08.195.
[21] Boodaghi Malidarre R, Akkurt I, Ekmekci I, Zakaly HM, Mohammed H. The role of La2O3 rare earth (RE) material in the enhancement of the radiation shielding, physical, mechanical and acoustic properties of the tellurite glasses. Radiat Eff Defects Solids. 2023;178(3–4):195–207. doi: 10.1080/10420150.2022.2113075.
[22] Boodaghi Malidarre R, Akkurt I, Zakaly HM. Investigation of Ag as chemical modifier in glassy SeTe chalcogenide alloy in terms of radiation shielding, optical, structural, and physical properties. Radiat Phys Chem. 2023;204:110685. doi: 10.1016/j.radphyschem.2022.110685.
[23] Boodaghi Malidarre R, Akkurt I, Kocar O, Ekmekci I. Analysis of radiation shielding, physical and optical qualities of various rare earth dopants on barium tellurite glasses: A comparative study. Radiat Phys Chem. 2023;207:110823. doi: 10.1016/j.radphyschem.2023.110823.
[24] Ilik E, Kavaz E, Kilic G, Issa SA, Zakaly HM, Tekin HO. A closer-look on Copper(II) oxide reinforced Calcium-Borate glasses: Fabrication and multiple experimental assessment on optical, structural, physical, and experimental neutron/gamma shielding properties. Ceram Int. 2021;48(5):6790–6801. doi: 10.1016/j.ceramint.2021.11.229.
[25] Reda SM, Saleh HM. Calculation of the gamma radiation shielding efficiency of cement-bitumen portable container using MCNPX code. Prog Nucl Energy. 2021;142:104012. doi: 10.1016/j.pnucene.2021.104012.
[26] Gunoglu K, Akkurt I. Radiation shielding properties of concrete containing magnetite. Prog Nucl Energy. 2021;137:103776. doi: 10.1016/j.pnucene.2021.103776.
[27] Bull JS, Kulesza JA, Josey CJ, Rising ME. MCNP® Code Version 6.3.0 Build Guide. Los Alamos National Laboratory Tech. Rep. LA-UR-22-32851, Rev. 1. Los Alamos, NM, USA: December 2022.
[28] ALMisned G, Sen Baykal D, Susoy G, Kilic G, Zakaly HM, Ene A, et al. Determination of gamma-ray transmission factors of WO3–TeO2–B2O3 glasses using MCNPX Monte Carlo code for shielding and protection purposes. Appl Rheology. 2022;32(1):166–77. doi: 10.1515/arh-2022-0132.
[29] Almatari M, Agar O, Altunsoy EE, Kilicoglu O, Sayyed MI, Tekin HO. Photon and neutron shielding characteristics of samarium doped lead alumino borate glasses containing barium, lithium and zinc oxides determined at medical diagnostic energies. Results Phys. 2019;12:2123–8. doi: 10.1016/j.rinp.2019.03.072.
[30] Tekin HO, ALMisned G, Susoy G, Ali FT, Baykal DS, Ene A, et al. Transmission factor (TF) behavior of Bi_2O_3–TeO_2–Na_2O–TiO_2–ZnO glass system: A Monte Carlo simulation study. Sustainability. 2022;14:2893. doi: 10.3390/su14052893.
[31] Tekin HO, ALMisned G, Rammah YS, Susoy G, Ali FT, Baykal DS, et al. The significant role of WO_3 on high-dense BaO–P_2O_3 glasses: transmission factors and a comparative investigation using commercial and other types of shields. Appl Phys A. 2022;128:470. doi: 10.1007/s00339-022-05620-y.
[32] ALMisned G, Bilal G, Baykal DS, Ali FT, Kilic G, Tekin HO. Bismuth (III) oxide and boron (III) Oxide substitution in bismuth-boro-zinc glasses: A focusing in nuclear radiation shielding properties. Optik. 2022;272:170214. doi: 10.1016/j.ijleo.2022.170214.
[33] Baykal DS, Kilic G, Ilik E, Kavaz E, ALMisned G, Cakirli RB, et al. Designing a Lead-free and high-density glass for radiation facilities: Synthesis, physical, optical, structural, and experimental gamma-ray transmission properties of newly designed Barium-borosilicate glass sample. J Alloy Compd. 2023;965:171392. doi: 10.1016/j.jallcom.2023.171392.
[34] ALMisned G, Günoğlu K, Özkavak HV, Baykal DS, Tekin HO, Karpuz N, et al. An investigation on gamma-ray and neutron attenuation properties of multi-layered Al/B4C composite. Mater Today Commun. 2023;36:106813. doi: 10.1016/j.mtcomm.2023.106813.
[35] Tekin HO, ALMisned G, Issa SAM, Zakaly HMH. A rapid and direct method for half value layer calculations for nuclear safety studies using MCNPX Monte Carlo code. Nucl Eng Technol. 2022;54:9. doi: 10.1016/j.net.2022.03.037.